AUTOMATED VOLUME SAMPLING OPTIMIZATION FOR DIRECT VOLUME DEFORMATION IN PATIENT-SPECIFIC SURGICAL SIMULATION

A. Kei Wai Cecilia Hung, B. Megumi Nakao, C. Kotaro Minato

Nara Institute of Science and Technology, Graduate School of Information Science
8916-5 Takayama, Ikoma, Nara, Japan

ABSTRACT

Patient-specific, interactive surgical simulation has become a major research direction in the biomedical side of computer graphics. While performing deformation on patients' medical volume data provides a realistic venue to define the most suitable operative strategy, the current simulators rely heavily on human efforts for data preprocessing. Such manual procedures not only require special knowledge from the users, they are tedious and time-consuming. This paper presents a novel volume sampling approach for preoperative planning by automating various conventional data preprocessing procedures. The optimization method is capable of adapting to any volume data and supports heterogeneous tissue characterization such that anatomical surroundings deform together with the deforming organ. In this way, physicians' user experience in surgical manipulation will be greatly improved. Results of the experiments suggested that the presented segmentation-free and modeling-free method is a more efficient and practical approach to interactive medical simulation.

Index Terms— Volume Visualization, Volume Deformation, Patient-specific Surgical Simulation, Optimization Methods, Automatic Preparation

1. INTRODUCTION

Ever since virtual reality came into the picture of the medical fields, surgical-related simulation became a prominent study as it provides safe and more accessible alternative methods of analyzing and collecting information as compared to mere observation or physically invasive examinations. Therefore, different applications such as [1, 2] are developed to achieve cost-effective and efficient preoperative planning and realistic surgical simulation.

In the survey of Soler and Marescaux [3], the surgical simulation throughout the course of volume visualization development can be summarized into two major milestones: the early virtual patient simulation and the more recent patient-specific simulations.

In a virtual patient simulation, due to early volume visualization techniques, each of the main anatomical structures has to be first segmented from the medical images. Afterwards, 3D modeling would be performed from the individual delineated structure to support manipulation, because such action would not be possible on a continuum rendered volume. Two works belonging to this category are done by Simone et al. [4] and De et al. [2]. Simone et al. developed a virtual cholangioscopy for bile duct stones diagnosis; while De et al. implemented a surgical training simulation on segmented models such as the liver and kidney gathered from the Visible Human Project.

The more recent concept of patient-specific simulator is to provide surgeons with the chance to perform the strategy on the "virtual copy" of the patient. So far, only a few works proposed applications [5, 6] with such capabilities using patient-specific data due to existing technical obstacles. Conventionally, several preparation steps should be completed manually by the developers before a patient-specific surgical simulation. Given a set of CT (Computed Tomography) or MRI (Magnetic Resonance Imaging) volume data which consists of medical images, the images are first reconstructed in the 3D environment in order to define the target area of manipulation or the region of interest (ROI). Secondly, a 3D anatomical model of the ROI in the form of a tetrahedral mesh, for instance, is generated. Thirdly, with the anatomical model, the corresponding physical conditions are assigned [7]. It is only after these steps that a physician can perform a surgical simulation.

As shown above, medical staffs are the end users of the simulation applications. Since many of the current simulators focus on canonical subjects consist of limited sets of preprocessed data, the medical staff can utilize the application without technical assistance. However, problem arises when these simulations set foot in the routine medical practice. Instead of the fixed subjects, the datasets used in the daily medical simulations are obtained from different individuals, making the simulations patient-specific. This characteristic implies very frequent change of data (every time a new patient's data is obtained). More than that, it also means going through the manual data preparation whenever the change happens. For the staffs that usually do not have any computer-related technical background, such procedures are unfriendly, tedious and time-consuming.

Currently, the subject of direct patient-specific volume manipulation has yet to be explored. Morris and Salisbury [8] are one of the few whose work is related to this subject. Their work presented a "pipeline of rapid preparation of deformable objects with no manual intervention". However, the starting point of the automation requires a segmented surface model of the target structure, which differs from the proposal of this paper on starting with original volume data.

This paper aims to present a new approach to automate the conventional data preprocessing procedures for real-time, patient-specific surgical planning simulation. At the same time, it also aims to facilitate the essential natural interactive deformation. With this approach, the concept of direct volume manipulation is demonstrated by hiding all preparation processes happening between loading the volume data to manipulating the rendered volume from the user's perspective. A volume sampling optimization by strategic vertex placement is proposed to portray the holistic characteristics of the volume data and the user's dynamic manipulation point, even in the absence of segmentation and modeling processes. Moreover, the vertices are brought to a novel usage of defining anatomical "deformable" and "non-deformable" regions. The algorithm was applied to a set of patient-specific kidney CT volume data and FEM-based deformation was evaluated. The result was compared against that of the volume sampling mesh without optimization. The

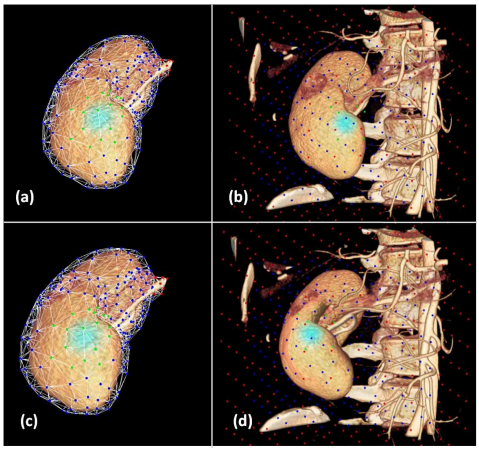

Fig. 1. (a & c) Conventional tetrahedral mesh before(a) and after(c) deformation; (b & d) Volume Proxy Mesh applied on a kidney CT volume data before(b) and after(d) deformation, note that the meshes define potential region of deformation

potential capability of the presented technique is evaluated.

Section 2 gives a discussion on the volume sampling mesh and the optimization algorithm. Section 3 presents the results of the optimization and its performance on interactive manipulation.

2. VOLUME SAMPLING OPTIMIZATION

This section describes the conceptual details and the step by step processes involved in the volume sampling optimization. First of all, the new idea of a volume sampling mesh, which is what this algorithm is optimizing, is briefly elucidated.

2.1. Volume Sampling Mesh

Volume sampling mesh is a novel concept of a tetrahedral mesh structure that contains vertices placed across the entire volumetric space. The vertices in a volume sampling mesh structure may come in all forms, may the vertices be regularly placed or randomly scattered. Unlike the conventional knowledge of a tetrahedral mesh where it is tailored to a segmented 3D structure, this mesh is non-object-specific (Fig. 1). As a result, it can handle volume manipulation of the entire image space.

The conceptualization of volume sampling mesh gives light to making direct volume manipulation a reality. By saying direct volume manipulation, it means that upon loading a volume dataset, a user may perform volume deformation once the objects are rendered in the virtual space. Since producing a volume sampling mesh does not entail any segmentation or modeling procedures, it can be applied to any volume dataset at any moment, without any form of manual intervention. In contrast to the current mesh preparation processes necessary as described in Section 1, the user would not even be aware of the presence of a mesh when the volume sampling mesh is applied for it is fully in the background. Therefore, this mesh is named as the "Volume Proxy Mesh" (VPM).

2.2. Optimized Volume Proxy Mesh

In a direct, patient-specific surgical simulation, it is the ideal case to produce quality, intuitive manipulation and deformation on the volumetrically rendered images with smooth interaction. A VPM would be an excellent approach to facilitate that. However, when the mesh is used in that context, there would be issues concerning the accuracy of the deformation and the computational efficiency. Consequently, optimizing the complexity of the VPM is needed in order to maximize its advantages.

To maintain smooth interactive performance, a small VPM vertex count is the most desirable. Since deformation quality relies heavily on the topology of the vertices in a mesh, strategic vertex placement across the 3D space in the optimized VPM is crucial to maintain a high degree-of-freedom around the ROI. This results to a tailored, optimized mesh that supports surrounding tissue deformation along with the manipulated organ.

Normally, vertices form on the surface a deformable organ to define boundaries. In this framework, nonetheless, the vertices are used to model the implicit geometries and the heterogeneous physical properties, such as the "deformable" and "non-deformable" areas. A "deformable" area contains objects that can be anatomically influenced by direct or indirect manipulation, for instance, fats, soft tissues, and blood vessels. Conversely, a "non-deformable" area pertains to objects that are anatomically uninfluenced by any manipulations, such as bones. This is particularly helpful to a realistic medical simulation.

The optimization algorithm can be described in four steps. The first two steps are fully automated data preprocessing that initially place vertices based on the image data. These two steps are performed in the background and thus there is absolutely no manual intervention. The latter two refine the initial vertex placements based on minimal user input during the simulation. Succeeding subsections below discuss about the details.

2.3. Algorithm Step 1: Vertex Evaluation

The first step of the optimization is vertex evaluation. This process is crucial as it directly determines the structure of the optimized mesh. To begin with, a set of dense, regularly distributed vertices is set across the whole volume data. This is to let the vertices sample the volumetric space thoroughly since dense vertices are capable of paying close attention to every small part of the volume data. Figure 2(a) is an example of regularly distributed vertices.

Afterwards, each of the distributed node is evaluated with a cost function given in equation (1):

$$C_{total}(v) = C_{intensity}(v)(w_g C_{gradient}(v) + w_d C_{density}(v)) \quad (1)$$

where v is a vertex in the 3D space at (x, y, z), $C_{total}(v)$ is the total cost of v, $C_{intensity}(v)$ is the intensity-based cost at $voxel(v)$, $C_{gradient}(v)$ is the gradient magnitude cost at $voxel(v)$, $C_{density}(v)$ is the density-based cost at v, and lastly w_g and w_d are weights of $C_{gradient}(v)$ and $C_{density}(v)$ respectively. Basically, the cost of vertex v describes the image data at voxel $v(x, y, z)$ and the relation of v with other vertices in three sub functions. Each of them is briefly discussed below.

2.3.1. Intensity based Cost Function

The intensity-based cost function is an intensity value based transfer cost function. In CT medical data, CT values are used to denote different bodily substances. The CT values, in turn, are represented in the intensity value of a voxel in a set of volume data. Therefore, the intensity value at a particular voxel can show which type of anatomical tissue a voxel has. With this background, the transfer function can focus on certain parts of the human body by assigning high cost

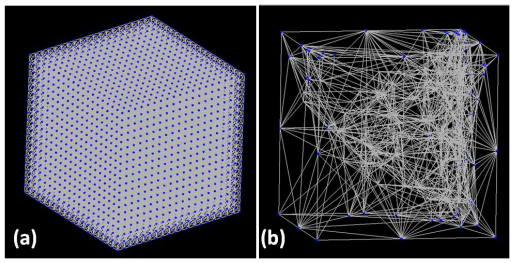

Fig. 2. (a) A set of dense vertices to sample the volume data in detail (b) Volume sampling mesh optimized to target vertex count: 250

to the vertex sampling the voxel. It is possible to accommodate user preferences for manipulation. Conversely, it can also avoid vertices from being placed on unimportant body parts.

2.3.2. Gradient based Cost Function

The gradient based cost function uses the gradient magnitude at $voxel(v)$. The higher gradient magnitude a voxel has, the higher indication that it is a volume boundary, thus higher chance of vertex being placed. This helps the algorithm to identify boundaries between objects and evaluate whether a vertex should be placed. The gradient magnitude of $voxel(v)$ is given by the first partial derivatives of the intensity value *I* with respects to $v(x, y, z)$, as shown in equation (2):

$$C_{gradient}(v) = |\nabla I| \;\; where \; \nabla I = \left(\frac{\partial I}{\partial x}, \frac{\partial I}{\partial y}, \frac{\partial I}{\partial z} \right) \qquad (2)$$

2.3.3. Density based Cost Function

The purpose of having density based cost function is to maintain the distribution of vertices over the volumetric space. As a well spread set of vertices would facilitate natural and stable volume deformation, this sub function serves as a form of balance to the previous two parts of the cost function. It is incorporated to prevent vertices from being overcrowded at one area while the rest is vise versa. The density based cost function is defined in equation (3):

$$C_{density}(v) = \sum_{j=0}^{n} \left(\frac{1}{|\mathbf{v}_i - \mathbf{v}_j|} \right) \qquad (3)$$

where the density of $voxel(v)$ is the sum of the distances of neighboring vertices v_j enclosed in a specified imaginary bounding sphere with vertex v_i as the center, as shown in Figure 3. The density cost of each affected vertex would be recalculated and changed whenever a vertex is removed.

2.4. Algorithm Step 2: Vertex Removal

The second step of the algorithm is vertex removal. After the vertex evaluation, all of the vertices are given a cost. From the original big number of dense vertices, this step eliminates one vertex with the minimum cost iteratively. For every vertex being removed, it would cause changes to vertex density of the neighboring vertices, therefore vertex density update for all affected vertices should be performed. Simultaneously, the final cost of the vertex will be updated as well. The process goes on and on, removing a vertex and updating changes

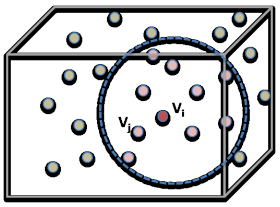

Fig. 3. Imaginary bounding sphere for density cost evaluation at vertex v_i to neighboring vertices v_j

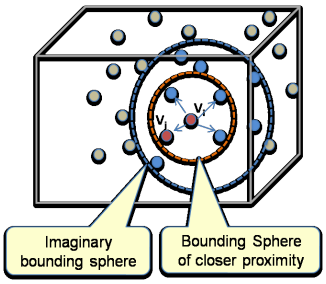

Fig. 4. Closer proximity bounding sphere, in addition to the imaginary bounding sphere for defining non-deformable area at vertex v_i

one by one, until the target vertex count is reached and step 2 terminates. By the end of this step, the set of initially placed vertices is generated. A sample of it is shown in Figure 2(b).

2.5. Algorithm Step 3: Deformable Area Definition

CT value information as a reference is applied in defining the non-deformable area. However, by relying purely on the CT value of a given voxel is not enough because of the gradual changing tissues around the same region. This step first recognizes vertices with CT values higher than a specified threshold to denote non-deformable tissue, and then it looks into the vertices' neighbors within a smaller proximity inside the imaginary bounding sphere (Figure 4). It is an assumption that the neighboring vertices of a non-deformable vertex with deformable CT values would be highly probable to be anatomically non-deformable too. In this approach, the neighboring vertices under such circumstances are "influenced" to convert into a part of non-deformable area as well. Though users may also specify which area to consider as non-deformable, the set of vertices is ready to produce an initial optimized mesh, without user's manipulation points.

2.6. Algorithm Step 4: Manipulation point based Refinement

Mesh refinement can be performed onto the initial optimized mesh by incorporating a user's region of manipulation. More than that, this process is meant to occur whenever the user switches to a new manipulation point. As the initial mesh is tailored to the volume data with only with few vertices only, pinpointing a manipulation point allows higher quality and degree of freedom in volume deformation. The refinement process can be done by adding more vertices to the existing initial mesh. According to the user's choice on the manipulation point of interest, additional vertices are defined and are merged as a part of the initial mesh based on the coverage range of the region of interest and the object boundaries within the regions.

At the end of this step, physicians can intuitively perform surgical simulation with the volume proxy mesh that is tailored to the

patient-specific data and the dynamically changing manipulation points.

3. SIMULATIONS AND RESULTS

This section examines the optimization results through the deformation performance of the proposed method for direct, patient-specific surgical simulations.

Throughout the optimization simulations, one consistent set of kidney CT volume data (256^3 voxels) was applied. All simulations began with a set of 8000 dense, regularly placed vertices and the goal of simulation was to reduce the vertex count significantly to 250. Since all of them are volume sampling meshes, their mesh generations were background processes as discussed. In deformation simulations, they were conducted using FEM-based deformation technique.

3.1. Volume Deformation

Figure 5(b-d) shows the comparison of the deformation result of the regularly placed Volume Proxy Mesh (Figure 5(b)), the initial optimized mesh (Step 2: Figure 5(c)) and manipulation-point-based refined mesh(Step 4: Figure 5(d)). In the simulations, same task of volume manipulation—pulling— with the same magnitude of force is applied to the blood vessel of the rendered kidney data.

Through the figures, it is observed that the deformation results became progressively articulate from the original rendered volume to the results of using manipulation-point-based refined mesh (Figure 5(a-d)). In particular, in Figure 5(d), the deformation result produced by the mesh that is optimized to the manipulation point has shown the highest-degree of freedom in detail-specific manipulation. Furthermore, aside from the deformation of the object of manipulation, it can be observed that the surrounding areas deformed along with the manipulation as well. This goes to show the importance of having vertices strategically placed when there are only a few vertices used in sampling the volume. While all the other sampling meshes made use of the same number of vertex count, the algorithm has fully maximized the vertex usage and produced an efficient yet natural-looking volume deformation environment.

3.2. Deformation Area Definition

Figure 5(e) and 5(f) has demonstrated the method to defining non-deformable area without manual intervention. As shown in Figure 5(e), initially the deformable vertices (yellow vertices) are along the supposedly non-deformable area—bone. However, when the non-deformable area definition was performed, most of the bone area became non-deformable (blue vertices). Thus, the approach is capable in supporting basic automated deformable and non-deformable area definition, later on incorporating human inputs to further enhance accuracy. To facilitate a believable heterogeneous surgical planning simulation, the mapping of physical parameters is essential.

4. CONCLUSION

This paper proposed a novel approach for direct patient-specific surgical simulation by automating conventional data preprocessing steps through volume sampling optimization. The framework first assigns dense vertices to sample the entire volumetric space before reducing the vertex complexity dramatically. The resulting mesh is not only tailored to specific patient data, it also supports heterogeneous tissue deformation in defining deformable and non-deformable areas. Simulations are performed based on the optimized results. Results have reconfirmed the need of having optimization for the volume sampling mesh. More than that, the proposed segmentation-free and modeling-free approach could be a practical method for direct, quality manipulation in a patient-specific simulation.

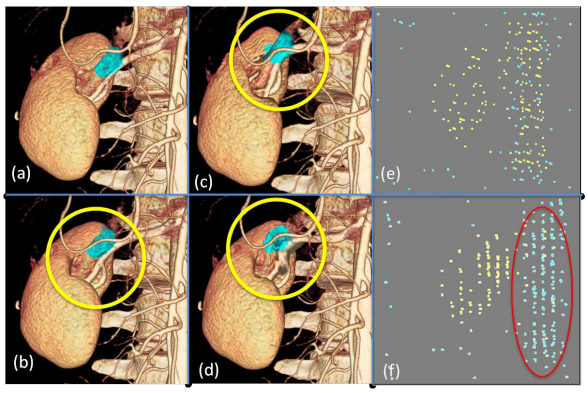

Fig. 5. Interactive volume deformation results based on: (a) Original rendered data, (b) Regularly placed volume sampling mesh, (c) Initial optimized mesh, (d) Manipulation-point-based refined mesh; Non-deformable area definition: (e) Before definition, (f) After definition

5. REFERENCES

[1] M. Nakao, T. Kuroda, H. Oyama, G. Sakaguchi, and M. Komeda, "Physics-based simulation of surgical fields for prooperative strategic planning," *Journal of Medical Systems*, vol. 30, pp. 271–380, October 2006.

[2] S. De, Y.-J. Lim, M. Manivannan, and M. A. Srinivasan, "Physically realistic virtual surgery using the point-associated finite field (paff) approach," *Presence: Teleoperators and Virtual Environments*, vol. 15, pp. 294–308, June 2006.

[3] L. Soler and J. Marescaux, "Patient-specific sugrical simulation," *World Journal of Surgery*, vol. 32, pp. 208–212, February 2008.

[4] M. Simone, D. Mutter, and F. Rubino, "Three-dimesional virtual cholangioscopy: a reliable tool for the diagnosis of common bile duct stones," *Annals of surgery*, vol. 240, pp. 82–88, 2004.

[5] S. Suzuki, K. Eto, and A. Hattori, "Surgery simulaion using patient-specific models for laparoscopic colectomy," *Studies in Health Technology Informatics*, vol. 125, pp. 464–466, 2007.

[6] Z. Cohen, J. Henry, D. McCarthy, V. Mow, and G. Ateshian, "Computer simulations of patellofemoral joint surgery. patient-specific models for tuberosity transfer," *American Journal of Sports Medicine*, vol. 31, pp. 87–98, January 2003.

[7] C. Basdogan, M. Sedef, M. Harders, and S. Wesarg, "Vr-based simulators for training in minimally invasive surgery," *IEEE Comput. Graph. Appl.*, vol. 27, pp. 54–66, March 2007.

[8] D. Morris and K. Salibury, "Automatic preparation, calibration, and simulation of deformable objects," *Computer Methods in Biomechanics and Biomedical Engineering*, vol. 11, pp. 263–279, June 2008.